WORKING PAPERS

N° 1755

June 2026

“Spatial accessibility indices in the framework of point processes. An application to veterinarian shortage”

Mehdi Berrada, Zaineb Smida and Christine Thomas-Agnan

Toulouse School of Economics

Spatial accessibility indices in the framework of point processes. An application to veterinarian shortage.

Mehdi Berrada [*] Zaineb Smida[†] Christine Thomas-Agnan [‡§]

June 14, 2026

Abstract

In a wide range of scientific fields, studying accessibility indices is essential for understanding how easily people can reach spatially distributed activities or resources, including employment opportunities, services, education, and, in particular, healthcare. Within the One Health framework, the health of humans, animals, and their shared environment is interdependent, making adequate veterinary care essential for safeguarding public health. The decline in the availability of veterinary healthcare in France adversely affects the health of food-producing animals. With this particular application in mind, and more broadly for supply-to-demand indices, we first reformulate the classical 2SFCA index within the framework of spatial point process theory and propose a new version that addresses its shortcomings. This enables us to define a population version of the classical as well as the new 2SFCA indices and to construct confidence bands for assessing their variability. In the application, we compute accessibility-to-veterinarian indices, and assess whether the spatial configuration of clinics and farms complies with a threshold recommended by the authorities.

Keywords: Accessibility, 2SFCA Index, Supply and Demand, Spatial Point Process, Veterinarian Shortage.

[*]UMR1219, Bordeaux Population Health, Inserm, University of Bordeaux, France, email: mehdi.berrada.1@u-bordeaux.fr

[†]Univ Lyon, INSA Lyon, UJM, UCBL, ECL, CNRS UMR 5208, ICJ, F-69621, France. Email: zaineb.smida@insa-lyon.fr.

[‡]Toulouse School of Economics, 1 Esp. de l'Université, 31000 Toulouse, France. Email: christine.thomas@tse-fr.eu.

[§]We acknowledge financial support from the French National Research Agency (ANR) under grants ANR-17-EURE-0010 (Investissements d'Avenir program).

1 Literature review

Among the precursors, Hansen (1959) pioneered the concept of accessibility in the field of city planning, describing it as the simplicity with which one can reach destinations from a particular location, utilizing either a specific travel mode or various available transport options. At the intersection of regional economics and urban geography, Weibull (1976) highlights the growing interest in quantitative methods for measuring accessibility to services and employment opportunities within urban regions. He presents an axiomatic framework rather than a specific indicator, establishing core axioms that accessibility measures should fulfill to ensure coherence and adaptability. Accessibility is defined not simply as spatial proximity between two points but rather as the reachability of a reference point to a set of multiple destinations.

In the literature of health geography, Guagliardo (2004) reviews the most popular indices of spatial accessibility to primary care, ranging from provider-to-population ratios to indices based on gravity models (spatial interaction models). One of the shortcomings of these latter models is that they are constructed using areal data. The shift from aggregate location-based indices to individual-centered measures of space occurred in the space-time framework in Kwan (1998) and represents a key evolution in accessibility measurement. Kwan (1998) showed that accessibility indices such as those derived from gravity models are valuable as indicators of place accessibility, but not for personal accessibility.

Luo and Wang (2003) pioneered the Floating Catchment Area (FCA) method, defining accessibility as a continuous measure indexed by a threshold distance (the size of the catchment) and showing that such measures are a special case of gravity-based measures. However, services within the catchment area are treated as equally accessible, while those outside are considered inaccessible. To improve upon this, Luo and Qi (2009) developed the enhanced two-step floating catchment area (E2SFCA) method, which assigns geographical weights to different zones according to distance, thereby accounting for distance decay and offering a more nuanced understanding of accessibility. A more recent extension (SDA-2SFCA) is introduced by Shao and Luo (2022) in the framework of health care, considering the heterogeneity of providers and the varying needs of patients.

Despite their positive evolution, these classical indices still present some drawbacks. In particular, they are all presented as empirical measures without any reference to a population parameter that they would estimate. As a consequence, one cannot measure their variability and cannot perform hypothesis testing. This is why we propose using statistical models of spatial point processes as a basis for construct-

ing new indices.

2 Gentle introduction to spatial point process theory

Spatial point processes provide a mathematical framework for modeling spatial point patterns (see Illian et al. (2008)). Heuristically, we can view a point process in a geographical area $W \subset \mathbb{R}^2$ as a random configuration of locations with a random number of points. The process is called simple when it is not possible to observe two points at the same location. In the case of supply and demand, we need two spatial point processes: one denoted by X for the locations of supplies with observed configurations $\{X_i, i \in \{1, 2...n^S\}\}$ and one denoted by Y for the locations of demand with observed configurations $\{Y_j, j \in \{1, 2...n^D\}\}$. In our application, supplies locations would be veterinarian clinics and demands locations would be farm's locations. A measure of the strength of the supply is provided by the number of working hours of veterinarians of a given clinic $\{m^S(X_i), i \in \{1, 2...n^S\}\}$ and the strength of the demand $\{m^D(Y_j), j \in \{1, 2...n^D\}\}$ can be proxied by the number of livestock units, a standardized reference unit used to aggregate heterogeneous animal stocks which reflect the farm's underlying demand for veterinary services. These two extra random variables attached to the locations are called marks in the spatial point process theory and a point process with marks is called a marked point process. The point process that includes only the spatial locations is called the ground process. In our case, these marks are positive random variables and we assume they are "independent marks", which means in this context that they are mutually independent conditionally on the ground process (but their distribution may depend on location).

Our index will be based on the first moments of these random variables (locations and marks) which are the spatial intensity of locations and the marked spatial intensity. Let us recall that for an unmarked point pattern Z with observed configuration $\{Z_i, i \in \{1, 2...n^Z\}\}$, the intensity is defined as follows. For a Borel subset B of $\mathbb{R}^2$, we first denote by $N_Z(B) = \sum_{i=1}^{n^Z} \mathbf{1}(Z_i \in B)$ the random number of points of Z belonging to B: N_Z is a random measure. The distribution of the process can be characterized by the total number of points $N_Z(W)$ and the conditional distribution of the locations given $N_Z(W)$. The intensity measure Λ_Z of Z is the measure given by the expected number of points

$$\Lambda_Z(B) = \mathbb{E}(N_Z(B)) \tag{1}$$

in a given Borel subset B. When this measure is proportional to the Lebesgue

measure, the proportionality factor represents the mean number of points per unit area. Otherwise, when this measure is absolutely continuous with respect to Lebesgue measure, it is given by

$$\Lambda_Z(B) = \int_B \lambda(x)dx, \tag{2}$$

where λ is called the intensity function (see e.g. Illian et al. (2008)) and describes how the mean number of points per unit area varies across space.

These definitions have been extended to marked processes by Schlather (2001) and Illian et al. (2008) in the homogeneous case and by Chiu et al. (2013) in the inhomogeneous case. See Bonneu and Thomas-Agnan (2015) for an application to economics. For a marked point process (Z, m_Z) with positive marks and observations $\{(Z_i, m_Z(Z_i)), i \in \{1, 2...n^Z\}\}$, the mark sum measure (also called marked intensity measure) is given by

$$\Lambda_{m_Z}(B) = \mathbb{E}\sum_{l=1}^{n^Z} m_Z(Z_l)\mathbb{1}\{Z_l \in B\}. \tag{3}$$

When this measure is absolutely continuous with respect to Lebesgue measure, the marked intensity function λ_{m_Z} (see Chiu et al. (2013)) is related to Λ_{m_Z} by

$$\Lambda_{m_Z}(B) = \int_B \lambda_{m_Z}(z)dz. \tag{4}$$

Noting that the case of the unmarked process is a particular case of the marked process by taking $m_Z(z) = 1$, we now provide a unique formula for both estimators of the intensity measure and intensity function.

The natural and unbiased estimator of the marked intensity measure of a Borel set B is just given by the sum of marks of points observed in B

$$\widehat{\Lambda}_{m_Z}(B) = \sum_{l=1}^{n^Z} m_Z(Z_l)\mathbb{1}\{Z_l \in B\}. \tag{5}$$

The marked-intensity function λ_{m_Z} of a spatial process Z can also be estimated by a non parametric estimator:

$$\hat{\lambda}_{m_Z}(z) = \frac{1}{b^2}\sum_{l=1}^{n^Z} m_Z(Z_l)K(\|Z_l - z\|/b), \tag{6}$$

where $b > 0$ is a bandwidth parameter and K a smoothing kernel density function satisfying $K(z) \geq 0, \forall z$ and $\int_A K(\|u\|)du = 1$. Note that the norm in (6) can represent simple Euclidean distance between the points or travel time in some applications. An edge correction may be added yielding

$$\hat{\lambda}_{m^Z}(z) = \frac{1}{b^2} \sum_{l=1}^{n^Z} w_l^{-1} m_Z(Z_l) K(\|Z_l - z\|/b), \tag{7}$$

where $w_l := \int_W \frac{1}{b^2} K(\|Z_l - x\|/b)dx$ and W is the total observation domain, see Bonneu and Thomas-Agnan (2015).

A variant of (5) is obtained by plugging in (4) a nonparametric estimator of the marked intensity like (6) or (7) yielding for example

$$\widehat{\Lambda}_{m_Z}(B) = \int_B \hat{\lambda}_{m_Z}(z)dz = \frac{1}{b^2} \sum_{l=1}^{n^Z} \int_B w_l^{-1} m_Z(Z_l) K(\|Z_l - z\|/b)dz, \tag{8}$$

where the edge correction may be omitted.

3 The classical 2SFCA index

After reformulating the classical 2SFCA index within a spatial point process framework to prepare for the transition to our new proposal, we explain its current limitations.

3.1 Recasting 2SFCA in the framework of spatial point processes

To facilitate the adaptation of the 2SFCA index, we will first present it using point process notations as in Section 2. Note that 2SFCA is directly presented in the literature as an empirical value computed from observations of the supply and demand processes and not as a characteristic of the distribution of these two processes as will be done in Section 4.

In Luo and Wang (2003), the 2SFCA index is presented in two steps for a given threshold distance r defining the catchment area:

- Step 1: For each supply location (clinic in our case) X_l, after identifying all demand locations Y_k that are within a distance r from X_l (representing the

catchment area for X_l), the local supply-to-demand ratio R_l is computed as follows:

$$R_l = \frac{m^S(X_l)}{\sum_{k=1}^{n^D} m^D(Y_k)\mathbb{1}\{\|X_l - Y_k\| \leq r\}}. \tag{9}$$

- Step 2: For each demand location Y_j, after identifying all supply locations X_l that are within a distance r from Y_j (representing the catchment area for Y_j), a sum of the local supply-to-demand ratios R_l at these locations is computed by:

$$I_j^{2SFCA}(r) = \sum_{l=1}^{n^S} R_l \mathbb{1}\{\|X_l - Y_j\| \leq r\} = \sum_{l=1}^{n^S} \frac{m^S(X_l)\mathbb{1}\{\|X_l - Y_j\| \leq r\}}{\sum_{k=1}^{n^D} m^D(Y_k)\mathbb{1}\{\|X_l - Y_k\| \leq r\}}. \tag{10}$$

3.2 Three shortcomings of the 2SFCA index

As already mentioned the first shortcoming of 2SFCA is that it remains an empirical index that does not have a population version.

A second shortcoming lies in the way the demands of farms and supplies of clinic are included in (10). Let us use a toy example to illustrate this problem, considering a configuration of clinics (red dots) and farms (blue dots) represented in Figure 1. Circles of radius r and centered at X_R, X_B and X_G, respectively, are represented around each of the three clinics (denoted by R for red, B for blue, and G for green) and around farm 1, which is the focus of our analysis here. The three lines in this Figure represent the limits of the Voronoï cells corresponding to the three clinics: they delimit the sets of points closest to each of the clinics, as can be seen in e.g. Aurenhammer (1991). The reason for this is explained further in this section.

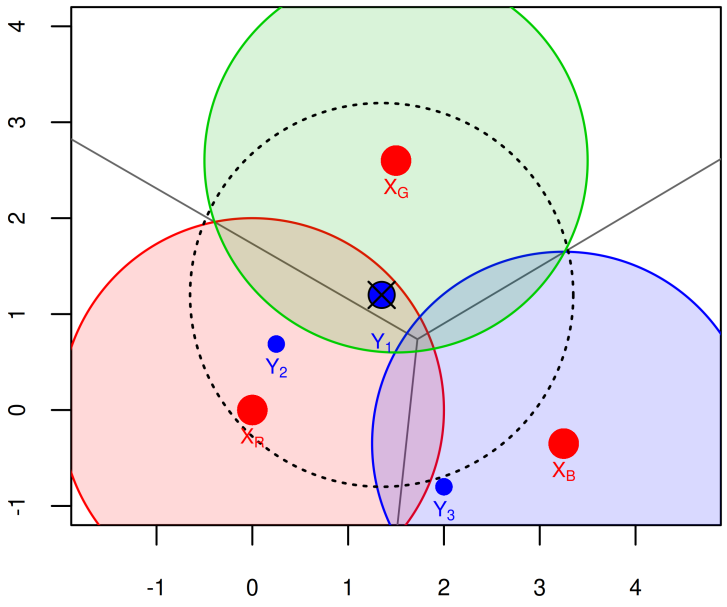

Figure 1: Toy configuration.

The local supply-to-demand ratio for the three farms are given by

$$R_R = \frac{m^S(X_R)}{m^D(Y_1) + m^D(Y_2)}, \qquad R_B = \frac{m^S(X_B)}{m^D(Y_3)}, \qquad R_G = \frac{m^S(X_G)}{m^D(Y_1)}.$$

Therefore we have for farm 1 located at Y_1, the only farm in the green disc,

$$I_1^{2SFCA}(r) = R_R + R_G = \frac{m^S(X_R)}{m^D(Y_1) + m^D(Y_2)} + \frac{m^S(X_G)}{m^D(Y_1)},$$

and for farm 2 located at Y_2, which is closer to the border of the red disc,

$$I_2^{2SFCA}(r) = R_R = \frac{m^S(X_R)}{m^D(Y_1) + m^D(Y_2)}.$$

We can see for example that the demand of point Y_1 appears in the denominator of R_R but also in that of R_V. This is because point Y_1 belongs to both catchment

areas of clinic R located at X_R and clinic G located at X_G. However even if farm 1 located at Y_1 has the possibility to visit both clinic R and clinic G, its demand should be divided into a part for clinic R and a part for clinic G instead of assigning the total to both clinics. This leads to bias downwards the index. Similarly on the numerator side as well, the supply of clinic R is fully dedicated to farm 1 whereas there could be a farm in the green disc but outside the blue circle that could benefit from this supply. In order to correct these flaws, we propose a simple allocation rule consisting in allocating a farm to its closest clinic. This allocation may not correspond to the actual choice of the farmer but, with a public policy point-of-view, all we care about is that there is enough supply for each farmer. This allocation rule avoids the problems mentioned above. This is the reason why we have pictured on Figure 1 the partition of the space with Voronoï cells.

Finally, the third shortcoming of the 2SFCA index is that, in the second step, the classical index attempts to aggregate the supply-to-demand ratios of clinics, or equivalently of the Voronoï cells, although this aggregation is not consistent with the nature of the variable being aggregated. Indeed, for a variable X defined on any subset Ω_k of a region Ω, and given a partition of Ω into K subsets Ω_k, we distinguish two cases:

- X is called extensive if $X_\Omega = \sum_{k=1}^{K} X_{\Omega_k}$
- X is called intensive if there exists weights w_k such that $X_\Omega = \sum_{k=1}^{K} w_k X_{\Omega_k}$.

For more information about these definitions, see Thomas-Agnan et al. (2015). An easy example to understand this concept is the following: the population variable is extensive, whereas the corresponding population density is an intensive variable, with weights given by the ratio of the area of Ω_k to the area of Ω. Supply-to-demand ratios are intensive variables. Therefore, a weighted aggregation formula should be used whose weights will be constructed from their denominator as explained in the next section.

4 Towards a new version of the 2SFCA index

We first justify the proposed modifications to the 2SFCA index. In the next section, we present several scenarios to illustrate the usefulness of these modifications. Finally, we define a version of the new index on any subarea of the domain without resorting to averaging empirical indices within subregion.

4.1 Definition of the new index

Let us denote by V_l the Voronoï cell associated with the clinic l located at X_l. Note that Voronoï cells have the property of containing exactly one clinic and forming a partition of the whole region. Each point y in the region belongs to a unique Voronoï cell.

In order to correct the second shortcoming of 2SFCA, we propose to use the Voronoï cells in the definition of the supply-to-demand ratio to avoid counting several times the same demand:

- in the numerator of the new ratio, we note that the supply of clinic l, $m^S(X_l)$ is also equal to the supply inside the intersection of $B(X_l, r) \cap V_l$ due to the allocation rule.
- in the denominator of the new ratio, we replace the demand within the ball of center X_l and radius r by the demand restricted to $B(X_l, r) \cap V_l$ because this results in the fact that each demand is counted exactly once (it is affected to its Voronoï cell).

This correction leads to the new version of the supply to demand ratio R_l^*

$$R_l^* = \frac{\hat{\Lambda}_{m^S}(B_l)}{\hat{\Lambda}_{m^D}(B_l)} = \frac{m^S(X_l)}{\hat{\Lambda}_{m^D}(B_l)}, \tag{11}$$

where $B_l = B(X_l, r) \cap V_l$ is the set of points in the ball $B(X_l, r)$ which are closest to clinic l and $\hat{\Lambda}_{m^S}$ (resp: $\hat{\Lambda}_{m^D}$) correspond to the natural and unbiased estimators of the marked-intensity measure of the supply (resp: demand) processes (see equation (5)), that is to say the total supply and demand in the intersection the of ball of radius r centered at clinic X_l and the Voronoï cell V_l.

In order to correct the third shortcoming, we aggregate these ratio while accounting for their intensive nature. For a farm j and a radius r, we consider the following partition of the relevant part of the space (i.e. clinics within a threshold of r kilometers from j)

$$\Omega_j(r) = \cup_{l:X_l \in B(Y_j,r)} B_l = \cup_{l:X_l \in B(Y_j,r)} B(X_l, r). \tag{12}$$

Indeed, for a given farm j and a given radius r, the only relevant clinics are those located within the ball $B(Y_j, r)$. Moreover, according to the allocation rule, only the part of their supply lying in the corresponding Voronoï cell V_l is taken into account. For example, in Figure 1, the region $\Omega_1(r)$ associated for farm 1 is the union of the green and the red areas.

Since the denominator of R_l^* is given by $\hat{\Lambda}_{m^D}(B_l)$ the aggregation weights for farm j are given by

$$w_l^* = \frac{\hat{\Lambda}_{m^D}(B_l)}{\hat{\Lambda}_{m^D}(\Omega_j(r))} \tag{13}$$

so that the aggregation yields

$$\begin{aligned} I_j^{2SFC2A*}(r) &= \sum_{l:X_l \in B(Y_j,r)} w_l^* R_l^* \\ &= \sum_{l:X_l \in B(Y_j,r)} \frac{\hat{\Lambda}_{m^D}(B_l)}{\hat{\Lambda}_{m^D}(\Omega_j(r))} \frac{\hat{\Lambda}_{m^S}(B_l)}{\hat{\Lambda}_{m^D}(B_l)} \\ &= \sum_{l:X_l \in B(Y_j,r)} \frac{\hat{\Lambda}_{m^S}(B_l)}{\hat{\Lambda}_{m^D}(\Omega_j(r))} = \frac{\hat{\Lambda}_{m^S}(\cup_{l:X_l \in B(Y_j,r)} B_l)}{\hat{\Lambda}_{m^D}(\Omega_j(r))} \\ &= \frac{\hat{\Lambda}_{m^S}(\Omega_j(r))}{\hat{\Lambda}_{m^D}(\Omega_j(r))}. \end{aligned} \tag{14}$$

Equation (14) allows to define a direct formulation for a population version of this index given by replacing the estimators by their population version, which finally corrects the first shortcoming of the classical index. For a given point y in the window of interest, the population version of the accessibility from y at radius r is given by

$$I_y^{2SFC2A*}(r) = \frac{\Lambda_{m^S}(\Omega_y(r))}{\Lambda_{m^D}(\Omega_y(r))} \tag{15}$$

where $\Omega_y(r)$ is defined by extending (12) to any location y (even if unobserved).

4.2 Some scenarios to compare the behavior of the new index with the classical version

Looking at formulas (10) and (14), we can describe as follows the difference between 2SFCA and 2SFCA*. On one hand, 2SFCA is the sum of ratios of supply in balls centered at clinics to demand in the same ball. On the other hand, 2SFCA* is the ratio of total supply within the union of these balls to total demand in the same area.

We now present some configurations for supply and demand to illustrate the advantage of the new approach. In all scenarios, the farms are represented by blue

points and the three clinics by red points. We also display the boundaries of the Voronoï cells. The balls of radius r around the clinics are colored respectively in green, red and blue, and the cross indicates the location of the farm we are focusing on for comparing the indices.

The difference between scenarios 1 and 2 is that one group of farms have migrated from $B(X_R, r) \cap B(X_G, r)$ to $B(X_R, r) \setminus B(X_G, r)$. Therefore the 2SFCA* remains stable since the farms which moved stayed in the same $\Omega_j(r)$ whereas 2SFCA has increased due to the fact that the denominator of the green clinic ratio has decreased.

Comparing scenarios 3 and 4, we see that the new index is stable at 0.222, whereas the classical 2SFCA index decreases from 1.111 to 0.222 when going from scenario 3 to scenario 4. However, the situation for our farm of interest should not change, because the only difference between the two scenarios is the location of the group of other farms within the red disc.

In scenario 5, the distribution of demand is even since the red and green clinics have 5 farms each while the blue has 4 but is out of reach of the central farm. Therefore 2SFCA* yields the ratio of $2/9 = 0.222$ whereas 2SFCA yields $\frac{1}{5} + \frac{1}{5} = 0.4$ overestimating the available supply.

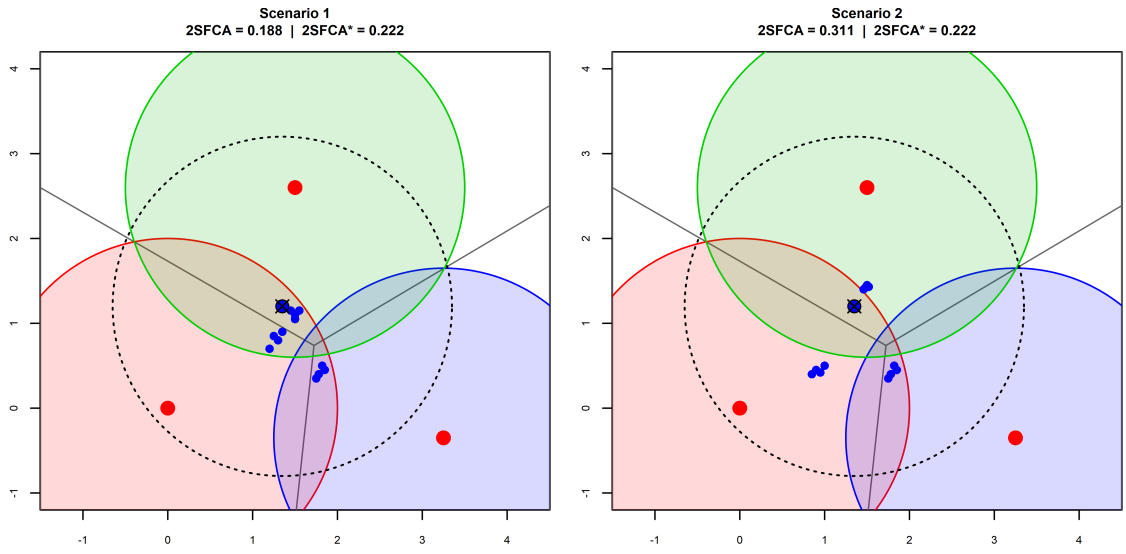

Figure 2: Scenarios 1 and 2.

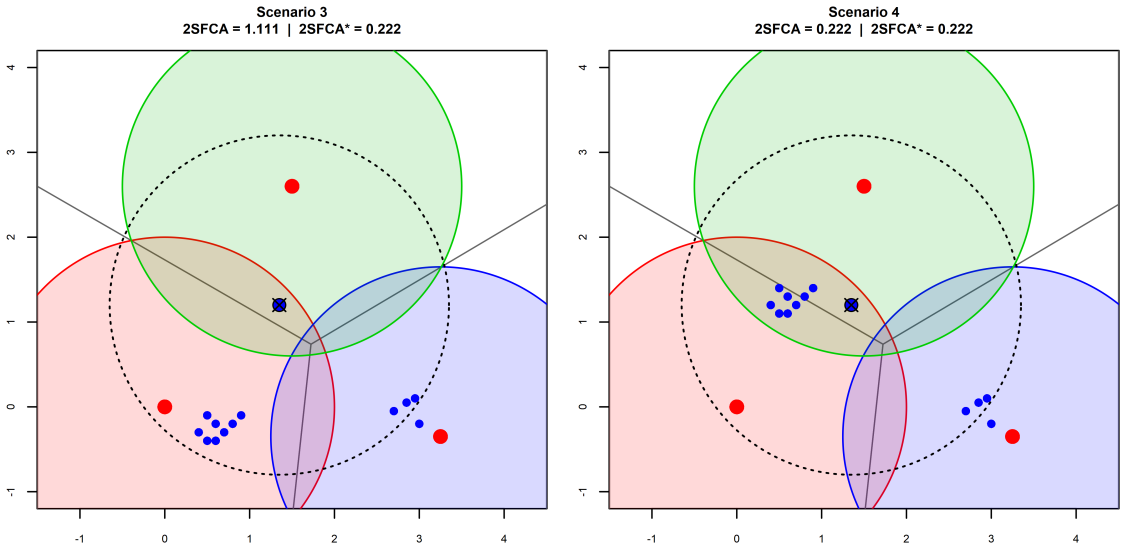

Figure 3: Scenarios 3 and 4.

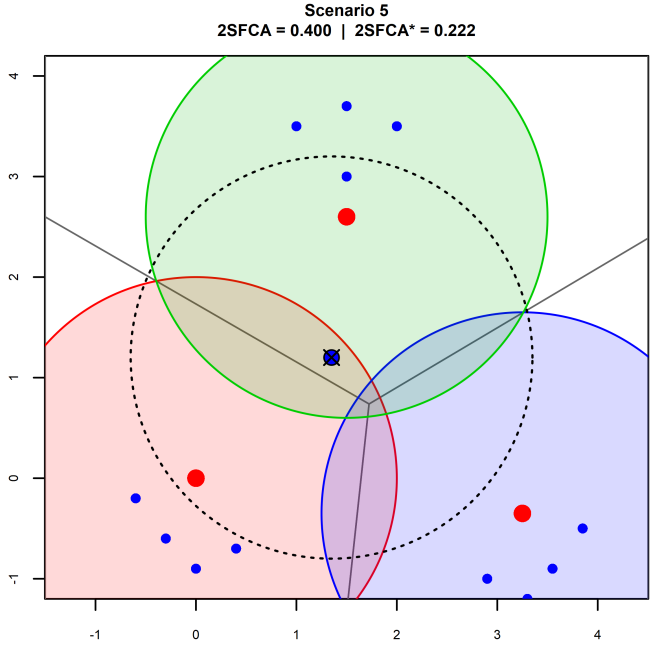

Figure 4: Scenario 5.

4.3 Areal version of the new index

First note that the classical 2SFCA is local in the sense that it is defined for a given demand location. When evaluating the inaccessibility of a subregion, the only solution is therefore to average the 2SFCA across the observed demand in this subregion. For our index 2SFCA* we now directly provide a global population (as well as a global empirical) version for a subregion.

Let $\Omega(r) = \cup_l B(X_l, r)$ be the set of locations in the observation window W which are at less than r kilometers from at least one clinic in W. Let B be a Borel set in W. It is now easy to define an areal version of the new index as follows:

$$I^{2SFC2A*}(B) = \frac{\Lambda_{m^S}(B \cap \Omega(r))}{\Lambda_{m^D}(B \cap \Omega(r))} \tag{16}$$

for the population version, and

$$\widehat{I^{2SFC2A*}}(B) = \frac{\hat{\Lambda}_{m^S}(B \cap \Omega(r))}{\hat{\Lambda}_{m^D}(B \cap \Omega(r))} \tag{17}$$

for the empirical one.

5 Data description

On the demand side, animal health care demand data come from the 2023 French National Bovine Database (BDNI), which exhaustively covers cattle farms only. Farms are geolocated using their geographic coordinates. Cattle characteristics are aggregated into Livestock Units (LU) in order to obtain a standardized and comparable measure of cattle populations across production types and ages. On the veterinarian supply side, the database is derived from the 2023 National Veterinary Order database and includes only practicing veterinarians. Professional addresses are geocoded to obtain geographic coordinates. To avoid overestimating effective cattle health care capacity, supply is measured using sector-specific full-time equivalents (FTE), which quantify the exact share of working time devoted to cattle rather than to other production sectors.

The study area encompasses the Centre-Val de Loire region, situated in central France, south of the Paris metropolitan area. This region provides a relevant case study due to its diverse livestock landscape and its contrasting veterinary demographics. The region shows a clear contrast in veterinary access (Figure 5): while the eastern part of the region maintains a stable access to veterinary services, the

western part is increasingly representative of the veterinary shortage phenomenon Berrada et al. (2022). Furthermore, the region is characterized by a dual production system, hosting significant populations of both dairy and beef cattle, which creates varied demands for healthcare. An analysis of the spatial distribution of veterinary full-time equivalents reveals a high intensity in the southern and south-eastern sectors of the region. In contrast to veterinary supply, the cattle distribution is more widely spread across the region, with high intensity in the south.

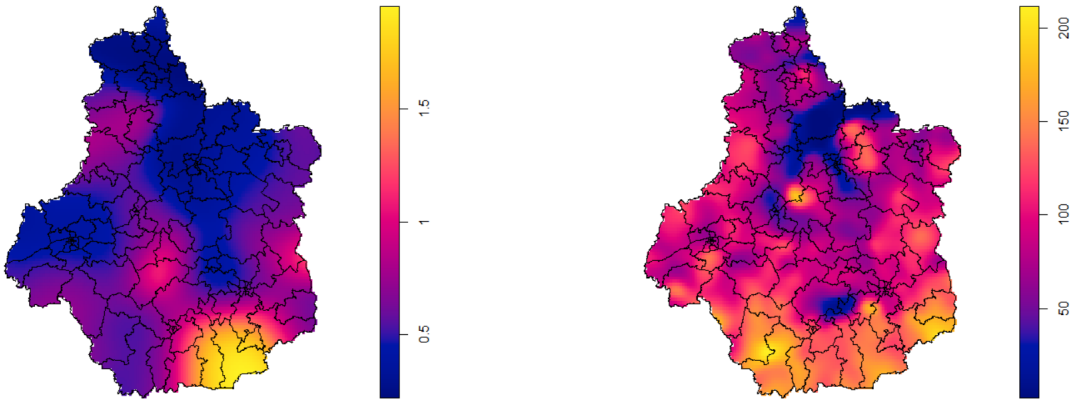

Figure 5: Spatial distribution of marked intensity of clinics (left panel) and farms (right panel).

The left panel of Figure 5 displays the kernel-based marked intensity of veterinary clinics, where marks correspond to full-time equivalent (FTE) veterinarians. The right panel shows the kernel-based marked intensity of livestock farms, where marks correspond to the Livestock Units (LU). Black lines denote the administrative boundaries of the cantons.

In an official decree, see French government (2021), the French Ministry of Agriculture and Food established standards for adequate veterinary coverage in the cattle sector. The decree specifies that common clinical procedures, prescribing activities, and drug administration are considered appropriately covered when at least one full-time equivalent (FTE) veterinarian is available per 5 000 livestock units (LU).

Another less restrictive norm specifies 1 FTE per 10 000 LU. For this reason we use in our computations a normalized version of the demand size multiplying the livestock units by 10 000 in the denominators of the indices so that the ratio of total supply to total demand is 1 when the less restrictive norm is obtained.

6 Results

In this section, we select the Centre-Val de Loire region to illustrate the comparison between the 2SFCA and its new version using real data. We then present a method to assess the variability of both indices.

6.1 Accessibility indices for Centre-Val de Loire

Still for the Centre-Val de Loire region, let us now picture the two accessibility indices for two different catchment radii.

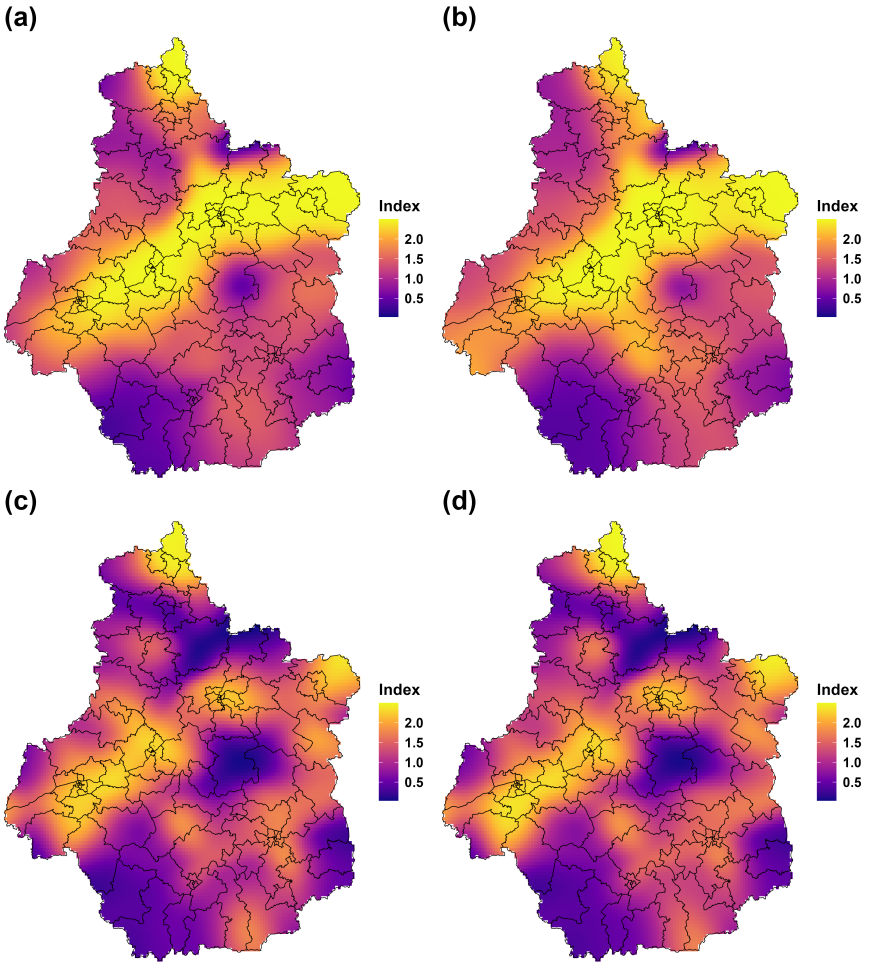

Figure 6: Veterinary health care spatial accessibility indices in Centre-Val de Loire: 2SFCA (left panel) and 2SFCA* (right panel).

Figure 6 illustrates the spatial distribution of accessibility indices. The top row uses a 30 km radius for **(a)** 2SFCA and **(b)** 2SFCA*; the bottom row uses a 15 km radius for **(c)** 2SFCA and **(d)** 2SFCA*. Black lines denote the administrative boundaries of the cantons. Although the intensity of veterinary supply is primarily concentrated in the south, both the 2SFCA and 2SFCA* indices reveal that this southern region exhibits a veterinary shortage (Figure 6). This suggests that in the southern area, veterinary supply remains insufficient relative to cattle demand, despite the high density of practitioners. The most well-endowed areas (highlighted in yellow) are not located in the south but instead form a diagonal stretching from the northeast

toward the center-southwest. The catchment radius r has some kind of smoothing effect when increased from $r = 15$ km (Panels a, b) to $r = 30$ km (Panels c, d), but the general pattern remains similar.

6.2 Variability assessment

In spatial point process theory, the variability of indices, like for example the Ripley's K function, is evaluated using Monte Carlo simulations of the process of interest. We follow the same strategy here by simulating the locations and the marks for the two processes as follows. We first estimate separately the location intensity functions of the two point processes. Then we simulate Poisson point processes with the obtained intensities, pretending they are independent. Conditionally on the locations, we generate the marks by randomly drawing a mark in the neighborhood of the location point (in the application, the neighborhood is defined by a circle of radius 30km). For each simulated set of locations and marks, we compute the 2SFCA* index on a grid of values of r, yielding a collection of simulated curves. The envelopes are obtained, for each radius, using the $95th$ and $5th$ percentiles of the empirical distribution of the observed indices at each given radius over the simulations.

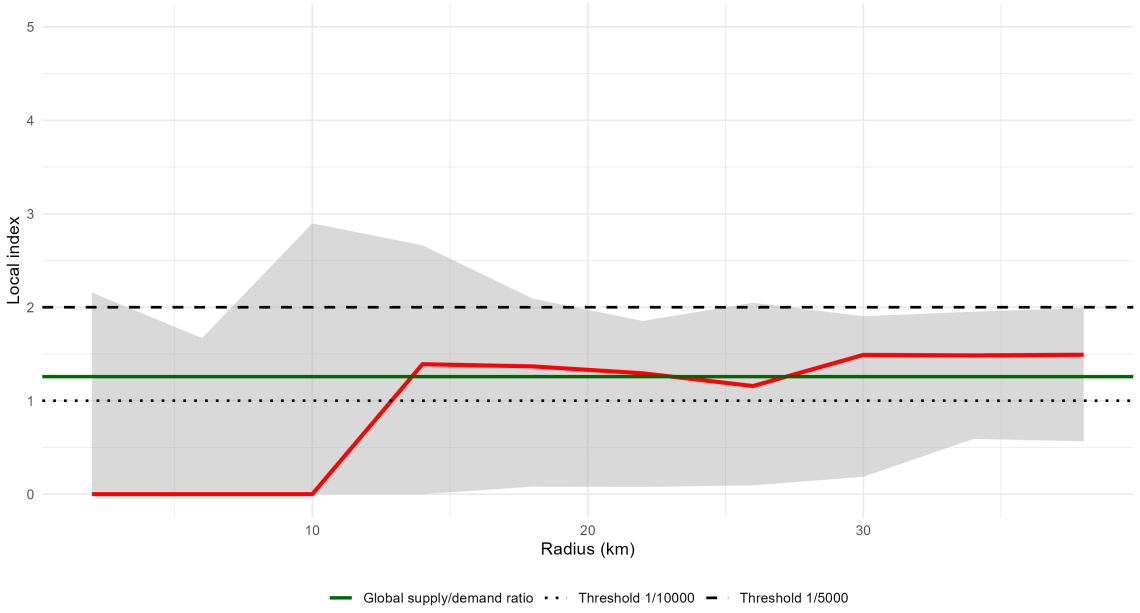

Figure 7: Simulation envelope for the 2SFCA* local accessibility index at a selected farm.

On Figure 7, the red curve represents the observed 2SFCA* index for a selected farm. The grey ribbon shows the 95% simulation envelope based on 50 realizations of an inhomogeneous Poisson process. The dark green line represents the regional supply-to-demand ratio. The two dashed lines indicate regulatory thresholds: 1 FTE per 5 000 LU (upper) and 1 FTE per 10 000 LU (lower).

For small catchment radii ($r < 10$km), the observed 2SFCA* index equals zero because no clinic lies within the catchment area of the selected farm. Around $r = 10$km, the index rises sharply as the first clinic enters the catchment, reaching a value close to the regional supply-to-demand ratio (green line). For larger radii, the observed index stabilizes and fluctuates around this regional average, remaining above the lower regulatory threshold (1 FTE per 10 000 LU) but consistently below the upper one (1 FTE per 5 000 LU). The upper bound of the envelope rarely exceeds this threshold, confirming that the veterinary shortage observed at this farm is unlikely to be driven by spatial configuration bias, but rather reflects a robust feature of the local supply–demand distribution.

7 Conclusion and perspectives

Using the framework of spatial point processes, we first propose a new accessibility index 2SFCA* based on relative marked intensity measures with an areal version on a subregion as well as a local version at a given demand location. This index is constructed by first identifying some shortcomings of the classical 2SFCA index, which we rewrite within this framework, and correcting them. The classical 2SFCA index has a single version which is empirical and local (for a given demand location). The proposed index 2SFCA* not only has a local empirical expression but also a local population version and an areal version adapted to measuring global accessibility within a subregion. The point process framework together with the population version allows us to construct confidence envelopes for the indices, which measure the variability of the indices. They are constructed using a simulation framework based on the assumption that the two ground processes are independent inhomogeneous Poisson with independent marks.

We then illustrate the comparison with a database of veterinary care supply and animal health care demand. Moreover, in this context, the fact that the data comply with the official recommendation of 1 veterinarian for 5000 animals translates into a simple inequality involving 2SFCA*.

Among the perspectives, we intend to improve the simulation framework by taking into account a possible correlation between the two ground processes. Another rather simple improvement would be to replace the empirical estimators of the in-

tensity measures with a smoothed version in the same spirit as Luo and Qi (2009) for 2SFCA.

References

Aurenhammer, F. (1991). Voronoi diagrams—a survey of a fundamental geometric data structure. *ACM computing surveys (CSUR)*, 23(3):345–405.

Berrada, M., Ndiaye, Y., Raboisson, D., and Lhermie, G. (2022). Spatial evaluation of animal health care accessibility and veterinary shortage in france. *Scientific reports*, 12(1):13022.

Bonneu, F. and Thomas-Agnan, C. (2015). Measuring and testing spatial mass concentration with micro-geographic data. *Spatial Economic Analysis*, 10(3):289–316.

Chiu, S. N., Stoyan, D., Kendall, W. S., and Mecke, J. (2013). *Stochastic geometry and its applications*. John Wiley & Sons.

French government (2021). Décret n° 2021-578 du 11 mai 2021 pris pour l'application du I de l'article L. 1511-9 du code général des collectivités territoriales et relatif aux aides aux vétérinaires contribuant à la protection de la santé publique et assurant la permanence et la continuité des soins aux animaux d'élevage. `https://www.legifrance.gouv.fr/jorf/id/JORFTEXT000043496356`. Accessed 01 June 2022.

Guagliardo, M. F. (2004). Spatial accessibility of primary care: concepts, methods and challenges. *International journal of health geographics*, 3:1–13.

Hansen, W. G. (1959). *Accessibility and residential growth*. PhD thesis, Massachusetts Institute of Technology.

Illian, J., Penttinen, A., Stoyan, H., and Stoyan, D. (2008). *Statistical analysis and modelling of spatial point patterns*. John Wiley & Sons.

Kwan, M.-P. (1998). Space-time and integral measures of individual accessibility: a comparative analysis using a point-based framework. *Geographical analysis*, 30(3):191–216.

Luo, W. and Qi, Y. (2009). An enhanced two-step floating catchment area (e2sfca) method for measuring spatial accessibility to primary care physicians. *Health & place*, 15(4):1100–1107.

Luo, W. and Wang, F. (2003). Measures of spatial accessibility to health care in a gis environment: synthesis and a case study in the chicago region. *Environment and planning B: planning and design*, 30(6):865–884.

Schlather, M. (2001). On the second-order characteristics of marked point processes. *Bernoulli*, pages 99–117.

Shao, Y. and Luo, W. (2022). Supply-demand adjusted two-steps floating catchment area (sda-2sfca) model for measuring spatial access to health care. *Social Science & Medicine*, 296:114727.

Thomas-Agnan, C., Vanhems, A., et al. (2015). Spatial reallocation of areal data–another look at basic methods. *Revue d'Économie Régionale & Urbaine*, (1):27–58.

Weibull, J. W. (1976). An axiomatic approach to the measurement of accessibility. *Regional science and urban economics*, 6(4):357–379.